The 9th European Congress on Computational Methods in Applied Sciences and Engineering
ECCOMAS Congress 2024
3 – 7 June 2024, Lisboa, Portugal

FLOW MANIPULATION STRATEGIES: DETACHED EDDY SIMULATION STUDY OF DBD PLASMA ACTUATORS IN A BLUFF BODY BURNER

F. BAGHERIGHGHAJARI*, J.C. PASCOA, M. ABDOLLAHZADEHSANGROUDI

* Universidade da Beira Interior, Departamento de Engenharia Eletromecânica, C-MAST—Center for Mechanical and Aerospace Sciences and Technologies,
Calçada Fonte do Lameiro, Covilhã, Portugal
e-mail: f.bagherighajari@ubi.pt , https://aerospace.ubi.pt/

Key words: Active flow control, electrohydrodynamic, flame stability, non-premixed combustion, plasma discharges.

Summary. *This study employs Detached Eddy Simulation (DES) to investigate the impact of Dielectric Barrier Discharge (DBD) plasma actuators on the control of non-reacting flow structures within a non-premixed bluff body burner. Plasma actuators were utilized in two operating modes: continuous and duty-cycled actuation. The objective is to assess the efficacy of these actuators in manipulating flow characteristics for enhanced combustion control. Numerical simulations were conducted to elucidate the interaction between plasma actuation and the turbulent flow around the bluff body burner by analyzing flow separation, vorticity dynamics, and overall flow structure. Our findings reveal that the plasma actuators significantly influence recirculation areas, demonstrating effectiveness in enhancing the mixing of fuel and oxidizer. The presence of the plasma actuators induces the formation of vortices, which slow down the flow movement and improve the interaction between the fuel and airflow streams, thereby promoting more favorable combustion conditions. The results also indicated an average 33% improvement in the spatial mixing for the steady actuation and 30% improvement in temporal mixing for the duty cycles operation. This study provides valuable insights into the mechanisms underlying plasma-based flow control, paving the way for further exploration in reactive flow environments.*

1 INTRODUCTION

Urgent actions must be taken in response to climate change, and transitioning to clean or green energy solutions is an inevitable choice. Eliminating the use of fossil fuels from the energy sector immediately is a very challenging task. Therefore, adopting technologies that aid the energy sector in transitioning to green energy solutions becomes a viable alternative for industries to reduce their emissions footprint and increase energy efficiency. In this regard, combustion of fossil fuels, which constitutes a major part of the energy sector, requires transitional solutions to improve combustion efficiency.

Surface dielectric barrier discharge (DBD) plasma actuators emerge as a novel option that has recently shown potential to improve combustion efficiency. DBD plasma actuators are active flow control devices that have been primarily used for subsonic aerodynamic flow

control applications, such as flow separation control, stall control, drag reduction, and boundary layer transition control [1]. These devices have a very simple structure, composed of two asymmetrically positioned electrodes (exposed and embedded) on either side of a dielectric layer. When an AC voltage with a sufficiently high amplitude and frequency is applied to the exposed electrode, the gases near the surface of the dielectric layer are ionized due to the high-intensity localized electric field. [2]. This local ionization of the gas results in the formation of a thin plasma zone. The gases experience a local body force and are accelerated in this region, leading to the formation of an ionic wind [3]. Besides this purely aerodynamic effect, some local surface and volume heating can also be observed in the surface plasma region [4]. This shows that surface DBD plasma actuators can have aerodynamic, local thermal, and gas decomposition effects on the working fluid, with the aerodynamic effect being the most significant. The use of plasma discharges in the combustion area is not new; several works have been reported in the literature on the application of plasma discharges for improving combustion efficiency [5]. In the majority of these cases, plasma discharges were used in volume discharge or arc discharge configurations with the aim of improving the ignition of the fuel/oxidant mixture or facilitating the chemical cracking and decomposition of combustion gases into more reactive components through processes known as plasma catalysis or plasma internal reforming. [6]. However, recent advancements in surface dielectric barrier discharge plasma actuators have opened up new avenues for combustion control using electrohydrodynamic-based active flow control devices. Im et al. [7] experimentally employed a DBD actuator to stabilize the base of a lifted ethane turbulent jet diffusion flame by modifying the co-flow velocity field. They integrated an axisymmetric DBD actuator onto the nozzle body, generating a directional flow that counteracted the surrounding co-flow around the jet nozzle. Their findings illustrated a significant reduction in the liftoff height of the turbulent jet diffusion flame due to this plasma actuation. Chen and Liao [8] conducted experimental investigations into flow interactions downstream of a bluff-body burner equipped with an annular plasma actuator. They showed that when the actuator was active, the jet at low Reynolds numbers became more prone to transitioning into turbulence, resulting in the formation of a vortex ring downstream of the bluff body. This phenomenon significantly enhanced flame stabilization. Chen and Liao[9] extended their previous work to the reacting flow regime of propane jet diffusion flames. Their results indicated that repetitive flame attachment could occur in the presence of the plasma-induced vortex ring. Mackay et al. [10] conducted a numerical simulation to evaluate the effectiveness of micron-scale field emission dielectric barrier discharge (FE-DBD) plasma actuators in non-premixed microburners. Across the simulated conditions, plasma actuation enhanced combustion completeness by improving mixing, generating radicals, and providing Joule heating. Li et al. [11] designed a swirler based on the dielectric barrier discharge (DBD) plasma actuator and demonstrated its effectiveness in controlling both jet flow and premixed jet flames. In their design, the plasma actuators were placed along the axial direction of the injector to induce a circumferential velocity in the main flow, creating a swirl tube. They showed that the swirl number could be adjusted by tuning the plasma actuator parameters. Li and Jiang [12] investigated the influence of electrical parameters on the characteristics of a plasma swirler, conducting both experimental and numerical analyses in a non-reacting flow regime. Their findings demonstrated that the swirl number increases almost linearly with electrode length.

The existing literature on simulations investigating the influence of DBD plasma actuators

on combustion is even scarcer than experimental studies. Wang an Roy[13], conducted a numerical simulation to investigate combustion stabilization and manipulation of recirculation zones inside a gas turbine combustor using serpentine plasma actuators. Their study demonstrated that the swirl generated by serpentine plasma actuators creates local low-velocity regions that stabilize the flame. Wang and Tsao [14] conducted computational studies on methane-air combustion using three configurations of plasma actuators placed around the periphery of a coaxial jet combustor. The study focused solely on the local body force exerted by the plasma near the combustor wall. Different flame structures were predicted based on the varying plasma configurations. Khasare et al. [15,16], conducted a two dimensional numerical study of the influence of the steadily operated annular DBD plasma actuators embedded on the surface the bluff body burner on the non-reacting and reacting flow field inside the burner. They demonstrated that plasma actuation aerodynamically modifies the recirculation zones to increase the mixing rate between fuel and oxidant. This adjustment reduces flame lift-off height and enhances the flame thickness root.

Various operating modes can be achieved by modulating the voltage waveform. The duty-cycled operating mode is created by a discontinuous AC voltage waveform characterized by two parameters: burst frequency ($F_\beta=1/T_{signal}$) and burst ratio ($\beta=T_{control}/T_{signal}$). The main characteristic of duty-cycled operation is the formation of discontinuous oscillatory wall jets that dissipate as counter-clockwise pulsating eddies. The discontinuous operation of the plasma actuator results in significantly lower power consumption compared to steady operation modes. Moreover, precise modulation of the duty cycle frequency and burst ratio can lead to enhanced performance by synchronizing the duty cycle frequency with the natural frequencies of the flow. Benard et al. [17] investigated the influence of surface plasma discharge actuators installed at the step corner of a backward-facing step. They conducted a parametric study varying the voltage magnitude, burst frequency, and duty cycle of the input voltage. Their findings revealed a minimum reattachment position of the separated flow when applying forcing at the shear layer mode at $St = 0.25$. Pouryoussefi et al.[18], conducted an experimental study on controlling flow around a backward-facing step using DBD plasma actuators. They demonstrated that the most effective method for exciting the shear layer is through unsteady actuation with an excitation frequency equal to the natural frequency of vortex shedding.

In this paper, we extend our previous study to include three-dimensional simulations and employ a scale-resolving turbulence model. This approach allows us to capture the influence and role of duty-cycled operation mode parameters on the non-reacting flow field downstream of a non-premixed bluff body burner. The study focuses on an annular DBD plasma actuator embedded on the surface of the bluff body.

2 MATHEMATICAL MODEL

The governing equations of the flow include continuity, momentum, and species transport equations, which are described by the averaged (or filtered) Navier-Stokes equations. It's important to note that our study specifically considers the non-reactive, isothermal flow regime inside the combustion chamber. The plasma actuator type under consideration is a non-thermal AC DBD plasma actuator, where the thermal power dissipation results in minimal temperature variation near the actuator surface[4]. Our focus here is solely on investigating the aerodynamic effects of the plasma actuator. Therefore, temperature variations inside the combustion chamber

are not considered, and the entire process is assumed to be isothermal. The Continuity, Momentum and species transport equations are respectively as follows:

$$\frac{\partial}{\partial t}(\rho) + \frac{\partial}{\partial x_i}(\rho u_i) = 0 \tag{1}$$

$$\frac{\partial}{\partial t}(\rho u_i) + \frac{\partial}{\partial x_j}(\rho u_i u_j) = -\frac{\partial p}{\partial x_i} + \frac{\partial}{\partial x_j}\left[\mu\left(\frac{\partial u_i}{\partial x_j} + \frac{\partial u_j}{\partial x_i} - \frac{2}{3}\delta_{ij}\frac{\partial u_k}{\partial x_k}\right)\right] + \frac{\partial}{\partial x_j}\left(-\rho\tau_{ij}^t\right) + \overrightarrow{f_b} \tag{2}$$

$$\frac{\partial}{\partial x_i}(\rho u_i Y_k) = -\frac{\partial}{\partial x_i}J_{k,i};\ \ k = CH_4, O_2, N_2\ with\ \vec{J}_k = -\left(\rho D_{i,m} + \frac{\mu_t}{Sc_t}\right)\nabla Y_i - D_{T,i}\frac{\nabla T}{T} \tag{3}$$

In the above Equation, Sc_t and μ_t are the turbulent Schmidt number and the turbulent viscosity. The mixture density ρ is also calculated using the ideal gas law. μ is the dynamic viscosity of the fluid and $\overrightarrow{f_b}$ represents the plasma-induced body force. In Equation (2), τ_{ij}^t is the residual stress tensor in LES framework or the Reynolds stress tensor in the case of RANS. Here, a the detached eddy simulation (DES) based on the realizable $k-\varepsilon$ model was chosen for the simulations. In this approach, the realizable $k-\varepsilon$ model is employed in the boundary layer, while adopting Large Eddy Simulation (LES) in the core turbulent region inside the burner where large unsteady turbulence scales dominate. We have chosen this hybrid approach to balance computational efficiency with accuracy. An examination of other hybrid LES-RANS turbulence models has been reported by Safavai and Amanai [19], where they concluded that the DES based on realizable $k-\varepsilon$ model would provide results with acceptable accuracy and reasonable run time for simulation of non-premixed combustion. In this model, equations (5) and (6) are solved for the kinetic energy of turbulence k and decay rate of the kinetic energy of turbulence ε [20]:

$$\frac{\partial}{\partial t}(\rho k) + \frac{\partial}{\partial x_i}(\rho k u_i) = \frac{\partial}{\partial x_j}\left[\left(\mu + \frac{\mu_t}{\sigma_k}\right)\frac{\partial k}{\partial x_j} - \frac{2}{3}\delta_{ij}\frac{\partial u_i}{\partial x_i}\right] + G_k + Y_k - \rho\varepsilon \tag{5}$$

$$\frac{\partial}{\partial t}(\rho\varepsilon) + \frac{\partial}{\partial x_i}(\rho\varepsilon u_i) = \frac{\partial}{\partial x_j}\left[\left(\mu + \frac{\mu_t}{\sigma_\varepsilon}\right)\frac{\partial \varepsilon}{\partial x_j} - \frac{2}{3}\delta_{ij}\frac{\partial u_i}{\partial x_i}\right] + \rho C_1\tilde{S}\varepsilon - \rho C_2\frac{\varepsilon^2}{k+\sqrt{v\varepsilon}} \tag{6}$$

In the above equations, G_k indicates the production rate of the kinetic energy of turbulence. The dissipation term Y_k in the k equation in the DES model is expressed by,

$$Y_k = \frac{\rho k^{\frac{3}{2}}}{l_{des}}\ \ with\ \ l_{des} = \min\left(\frac{k^{\frac{3}{2}}}{\varepsilon} + C_{des}\Delta\right) \tag{7}$$

In the above, C_{des} is a calibration constant with a value of 0.61 and Δ is the maximum local grid spacing ($\Delta x, \Delta y, \Delta z$). To calculate the volumetric body force induced by the plasma actuator $\overrightarrow{f_b}$, a simple phenomenological model for the DBD plasma actuator is considered [21]. This model is similar to the one proposed by Suzen et al. [22]. The two basic equations of this model are as follows:

$$\nabla.(\epsilon_r\nabla\phi^*) = 0 \tag{8}$$

$$\nabla.(\epsilon_r\nabla\rho_c^*) = -\frac{\rho_c^*}{(\lambda_d)^2} \tag{9}$$

In the above relations, ϕ^* represents the normalized electric potential and also ρ_c^* shows the normalized charge density distribution near the surface of the actuator. In these equations, λ_d and ϵ_r represent the Debye length and relative dielectric permittivity. By solving Equations (8)

and (9), the plasma-induced volume force can be calculated based on normalized electric potential and charge density as follows:

$$\vec{f_b} = \rho_c \vec{E} = \rho_c^{max} \phi^{max} f^2(t) \rho_c^* (-\nabla \phi^*) \tag{10}$$

In the above, $f(t)$ is the wave function, ϕ^{max} is the amplitude of applied voltage, and ρ_c^{max}represents the highest electric charge density. The value of ρ_c^{max} controls the intensity of the plasma discharge and serves as an input parameter for the model. For a steady-state solution, the wave function can be considered as a square wave function [23]. In this case, $f^2\ (t)$ will be equal to unity. The value of ρ_c^{max} should be determined such that it accurately captures the nonlinear dependency of the plasma-induced body force on the applied voltage.

3 PROBLEM DESCRIPTION AND BOUNDARY CONDITIONS

The schematic representation of the non-premixed bluff body burner with an annular plasma actuator embedded on the surface of the bluff body is shown in Figure 1. On the surface of the bluff body, the annular dielectric barrier discharge (DBD) plasma actuator is strategically configured to generate an outward jet directed towards the airflow stream. The dimensions of the bluff body burner and the plasma actuator are given for simplicity in a two-dimensional cross-section of the geometry in Figure 1c.

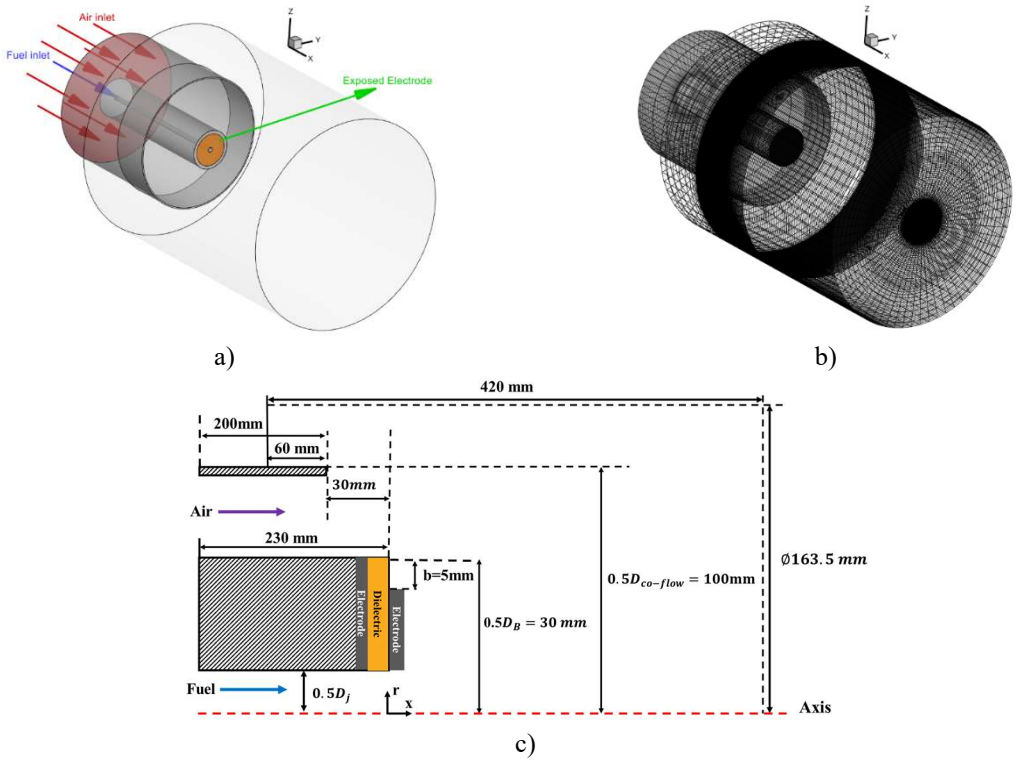

Figure 1: Schematic representation of the plasma actuator embedded bluff body burner and the mesh.

Air and fuel enter the computational at a uniform speed. At the inlet boundaries, the value

of k and ε is estimated based on the turbulence intensity. In the model governing equations for the DBD plasma actuator, specific boundary conditions are required for electric potential and charge density. Electric potential is applied to the injecting electrode (exposed electrode) with an amplitude of 12 kV. The normalized charge density distribution is applied as follows on the part of the surface of the dielectric material that covers the embedded electrode:

$$\rho_{c,w}^{*} = G(s) = exp\left[-\frac{(s-\xi)^2}{2\gamma^2}\right] \tag{11}$$

4 NUMERICAL PROCEDURE AND VALIDATION

The numerical simulation is performed using Ansys Fluent, where the governing equations for the phenomenology of the plasma actuator are incorporated using user-defined functions (UDFs). The grid was created in such a way to provide adequate resolution for the plasma region and sufficient resolution of the turbulent kinetic energy spectrum. The time step for the flow simulation was also selected to maintain a Courant number less than unity, ensuring numerical stability and accuracy throughout the simulation

For the validation purposes, two specific cases are considered. The first validation case involves studying the flow induced by an annular DBD plasma actuator under quiescent conditions. The second validation case focuses on the non-reacting flow field inside an isothermal non-premixed burner. we have used the model the same modeling approach as presented in section 2 and tuned the parameters of the plasma model (The charge density and the shape factor) to obtain the best fit with results reported by Borradaile et al [24] as shown in Figure 3a. For the second validation case, the non-reacting flow field inside a non-premixed bluff body burner is simulated and the results are compared with the experimental results of Tong et al [25].

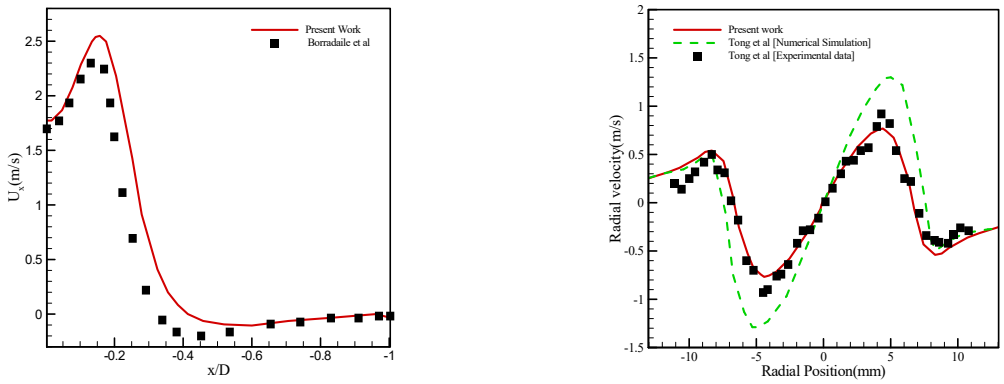

Figure 3: Comparison of a) the velocity profile induced by the annular DBD plasma actuator with the results reported in [24] and b) the velocity profile inside a non-premixed bluff body burner with the results of [25].

5 RESULTS AND DISCUSSION

The vorticity magnitude contours inside the burner for various operating conditions of the plasma actuator are shown in Figure 4. In this figure F^{+} signifies the reduced duty cycle frequency which is defined as the ratio of the duty cycled frequency to the Reffrence

characteristic frequency of the problem (calculated based on the inflow velocities and the bluff body dimeter as 256Hz). According to these figures, in the case without the plasma actuator, the jet penetration is longer, and the width of the recirculation zone is smaller. In our previous 2D asymmetric simulation of the non-premixed bluff body burner, we demonstrated that the size of the cavity created by the recirculation zone directly influences the size of the cavity formed in the flame structure. In other words, the size of the recirculation zone affects the flame lift-off height. When the plasma actuator is activated, the jet penetration length is significantly reduced, and the width of the recirculation zones increases. The reduction in jet penetration length indicates that the mixing zone is closer to the bluff body surface. In the case of a reacting regime, this would suggest that the flame is likely to be positioned closer to the bluff body surface. For the duty-cycled cases, the plasma effect also results in a reduction of the jet penetration length. The influence of duty-cycled operation improves with an increase in burst frequency. Conversely, when the burst ratio is reduced, the duty cycle exhibits a weaker influence on the flow structure.

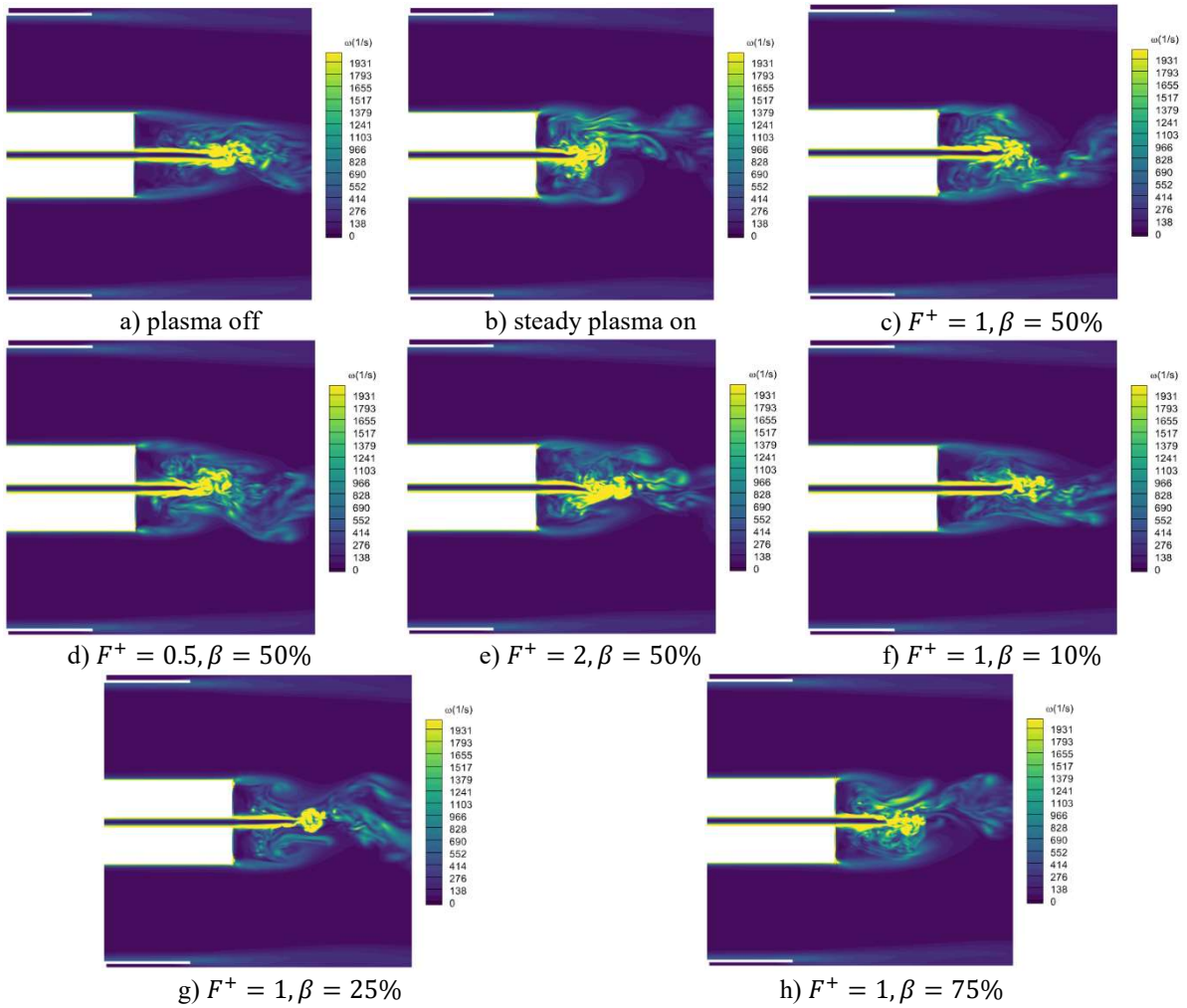

Figure 4: Instantaneous vorticity magnitude contours.

The time-averaged flow streamlines and velocity magnitude contours for various operating

cases of the plasma actuator are shown in Figure 5. These figures exhibit similar behavior to those in Figure 4, but from a time-averaged perspective. The general trend indicates that when the plasma actuator is active, the elongation of the recirculation zones is reduced, and the zones become thicker.

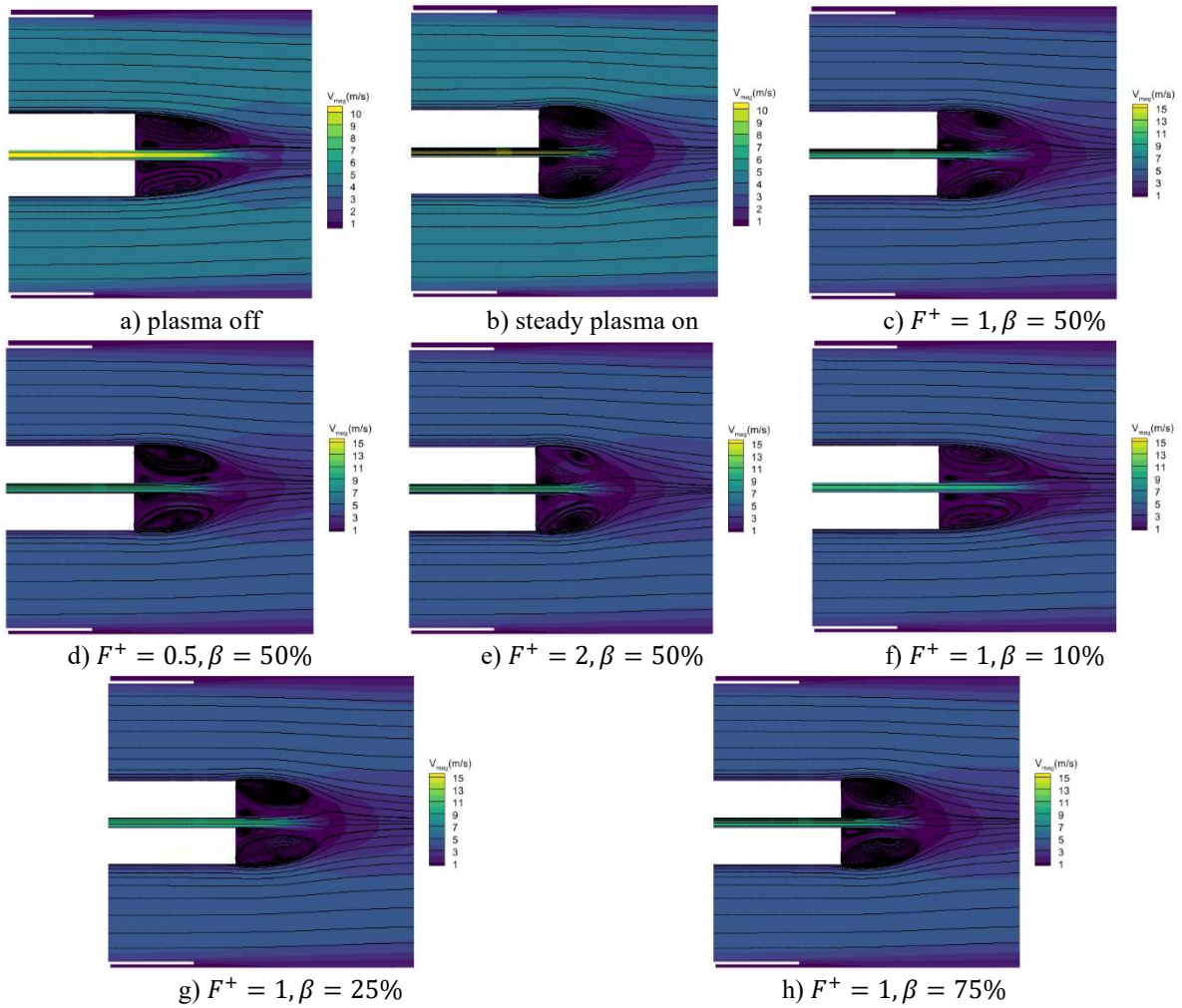

Figure 5: Time averaged velocity magnitude contours and flow stream lines.

To conduct a frequency analysis of the flow domain, four numerical probes are considered. The coordinates of these probes are provided in Table 1. The locations of these probes are strategically selected to characterize the frequencies of the outer and inner shear layers, as well as the internal and external recirculation zones. The pressure variation over time at each of these probes is recorded, and the signal is processed using a Fast Fourier Transform (FFT) to convert it to the frequency domain.

Table 1: Coordinates of the numerical probes.

Probe number	x/D	y/D
P1	0.03	0.023
P2	0.0097	0.0019

P3	0.057	0.0096
P4	0.0035	0.036

The power spectral density versus the frequency domain at various probes and for different operating modes of the plasma actuators is plotted in Figure 6. A notable observation is that for all cases where the plasma actuator is active, the amplitude of the flow oscillations increases significantly (see the scale of the vertical axis). For the duty-cycled cases, the amplitude of flow oscillations is visibly enhanced at frequencies above 50 Hz. The variation of the reduced duty-cycled frequency (F^+) shows that in the case with $F^+ = 0.5$ the high-frequency oscillations systematically extend to lower frequency ranges, reaching as low as 100 Hz compared to other two cases of $F^+ = 1, 2$.

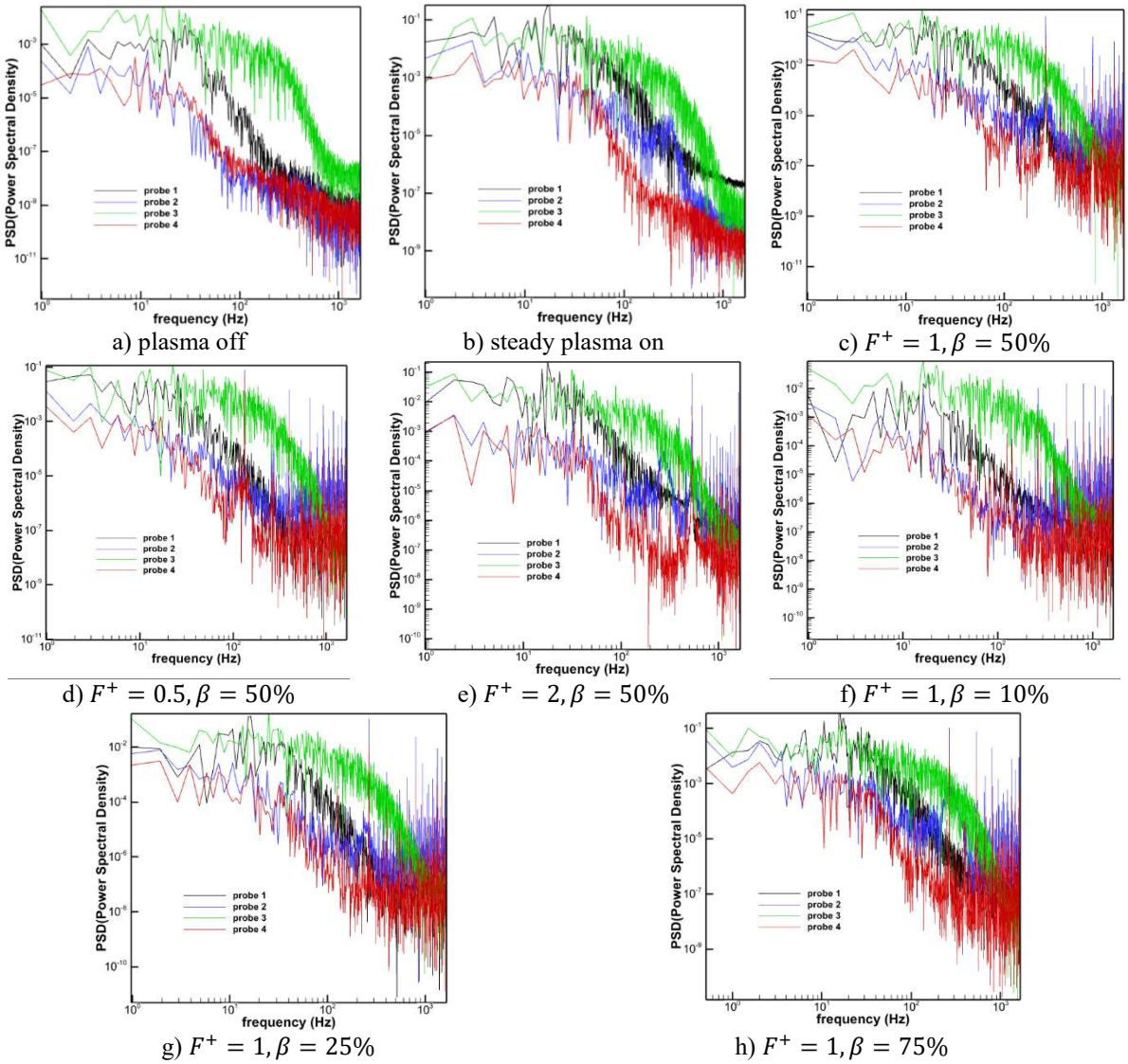

a) plasma off b) steady plasma on c) $F^+ = 1, \beta = 50\%$

d) $F^+ = 0.5, \beta = 50\%$ e) $F^+ = 2, \beta = 50\%$ f) $F^+ = 1, \beta = 10\%$

g) $F^+ = 1, \beta = 25\%$ h) $F^+ = 1, \beta = 75\%$

Figure 6: FFT analysis of the pressure signals.

The Spatial Mixing Deficiency (SMD) index[26], and the Temporal Mixing Index (TMD)

(TMD) are used to quantify the mixing efficiency, which are defined as follows:

$$SMD = \frac{\sqrt{AVG_{plane}\left\{\left(<C_F>-AVG_{plane}(<C_F>)\right)^2\right\}}}{AVG_{plane}(<C_F>)} \times 100\ (\%) \tag{12}$$

$$TMD = AVG_{plane}\left\{\frac{\sqrt{<((C_F-<C_F>)^2>}}{<C_F>}\right\} \times 100\ (\%) \tag{13}$$

In the above equation, C_F is the molar concentration of fuel and $AVG(C_F)$ stands for the average value of C_F. SMD is a measure of the spatial heterogeneity of the time-averaged flow quantity, whereas TMD is a spatial average of the temporal heterogeneity at various points over a plane [27] . A smaller SMD or TMD indicates better mixing [28]. The variation of SMD is calculated using cross-sectional planes with a diameter of 90 mm along the axis of the burner. This diameter is selected to represent the volume encompassing the flame structure. We have also calculated the TMD values. For the calculation of the TMD, cross-sectional planes with a diameter of 60 mm along the axis of the burner were used. This smaller diameter was chosen to avoid division by zero. The variation of the SMD along the axis the burner is plotted in Figure 7. As shown, the SMD values decrease for all cases due to plasma actuation, indicating improved mixing of the fuel and oxidant. The results in this figure demonstrate that steady plasma actuation with an applied voltage of 10 kV has a more pronounced effect on enhancing mixing.

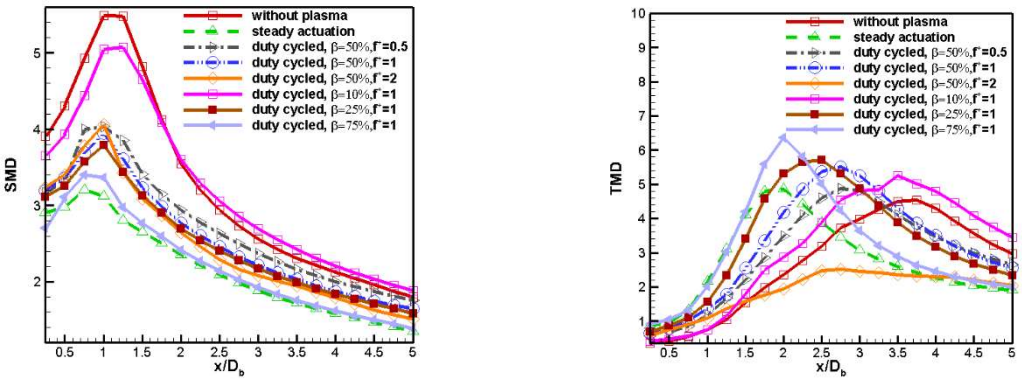

a) b)

Figure 7: Variation of the a) SMD and b) TMD along the axis of the burner.

6 CONCLUSIONS

In this paper, the influence of the duty cycled DBD plasma actuator mounted in the surface of a non-premixed bluff body burner was simulated. The influence of the actuator on the no-reacting flow fields and the recirculation zones downstream of the bluff body was analyzed for various duty cycle frequency and burst ratios. The mixing efficiency of the duty cycled plasma actuator was also analyzed using spatial and temporal mixing deficiency parameters. The most important results can be summarized as:

- When the plasma actuator is active, the jet penetration length is significantly reduced, and the width of the recirculation zones increases.
- the amplitude of the flow oscillations increases significantly for plasma on cases.

- The amplitude of the flow oscillations increases significantly for plasma on cases and duty plasma actuation improved the mixing between fuel and oxidant as shown by the reduction in the SMD and TMD values.

ACKNOWLEDGMENTS

F. Bagherighajari acknowledges Ph.D. scholarship with the reference number 2022.09877.BD from FCT-Foundation for Science and Technology and the support by Portuguese national funds by FCT, within the unit C-MAST - UIDB/00151/2020 (https://doi.org/10.54499/UIDB/00151/2020) and UIDP/00151/2020 (https://doi.org/10.54499/UIDP/00151/2020).

REFERENCES

[1] M. Abdollahzadeh, F. Rodrigues, J.C. Pascoa, P.J. Oliveira, Numerical design and analysis of a multi-DBD actuator configuration for the experimental testing of ACHEON nozzle model, Aerosp. Sci. Technol. 41 (2015) 259–273.

[2] M. Abdollahzadeh, F. Rodrigues, J.C. Pascoa, Simultaneous ice detection and removal based on dielectric barrier discharge actuators, Sensors Actuators A. Phys. 315 (2020) 112361.

[3] N. Amanifard, M. Abdollahzadeh, H. Moayedi, J.C. Pascoa, An explicit CFD model for the DBD plasma actuators using wall-jet similarity approach, J. Electrostat. 107 (2020) 103497.

[4] F. Rodrigues, J. Pascoa, M. Trancossi, Heat generation mechanisms of DBD plasma actuators, Exp. Therm. Fluid Sci. 90 (2018) 55–65.

[5] L. Fei, B.B. Zhao, Y. Chen, L.M. He, Z.C. Zhao, J.P. Lei, Rotating gliding arc discharge plasma-assisted combustion from ignition hole, Exp. Therm. Fluid Sci. 129 (2021) 110473.

[6] R. Yang, X. Che, B. Deng, Y. Lin, Dielectric barrier discharge plasma reforming of methane in rocket engine: Characteristics and technical feasibility, Int. J. Hydrogen Energy. 61 (2024) 238–250.

[7] S.K. Im, M.S. Bak, M.G. Mungal, M.A. Cappelli, Plasma actuator control of a lifted ethane turbulent jet diffusion flame, IEEE Trans. Plasma Sci. 41 (2013) 3293–3298.

[8] J.L. Chen, Y.H. Liao, Effects of an annular plasma actuator on a co-flow jet downstream of a bluff-body, Appl. Therm. Eng. 192 (2021) 116975.

[9] J. Chen, Y. Liao, Influence of a plasma actuator embedded in a bluff-body on the stabilization of nonpremixed jet flames, Int. J. Heat Fluid Flow. 100 (2023) 109111.

[10] K.K. MacKay, H.T. Johnson, J.B. Freund, Field-emission plasma enhancement of H2–O2 micro-combustion, Plasma Sources Sci. Technol. 29 (2020) 045014.

[11] G. Li, X. Jiang, Y. Zhao, C. Li, Q. Chen, G. Xu, et al., Jet flow and premixed jet flame control by plasma swirler, Phys. Lett. A. 381 (2017) 1158–1162.

[12] G. Li, X. Jiang, Effects of electrical parameters on the performance of a plasma swirler, Phys. Scr. 94 (2019) 095601.

[13] C. Wang, S. Roy, Numerical simulation of a gas turbine combustor using nanosecond pulsed actuators, in: AIAA 2013-0894, 2013: pp. 1–17.

[14] C. Wang, H. Tsao, Control of a Turbulent Non-Premixed Flame by Plasma Actuators, J. Thermophys. Heat Transf. 32 (2018) 111–117.
[15] S. Khasare, F. Bagherighajari, F. Dolati, J. Mahmoudimehr, J. Páscoa, M. Abdollahzadehsangroudi, The effect of the dielectric barrier discharge plasma actuator in the control of non-reactive flow in a non-premixed bluff body burner, Phys. Fluids. 35 (2023) 075135.
[16] S. Khasare, F. Bagherighajari, F. Dolati, J. Mahmoudimehr, J.C. Pascoa, M. Abdollahzadeh, Control of the flame and flow characteristics of a non-premixed bluff body burner using dielectric barrier discharge plasma actuators, Appl. Therm. Eng. 235 (2023) 121432.
[17] N. Benard, P. Sujar-Garrido, J.P. Bonnet, E. Moreau, Control of the coherent structure dynamics downstream of a backward facing step by DBD plasma actuator, Int. J. Heat Fluid Flow. 61 (2016) 158–173.
[18] S.G. Pouryoussefi, M. Mirzaei, M. Hajipour, Experimental study of separation bubble control behind a backward-facing step using plasma actuators, Acta Mech. 226 (2015) 1153–1165.
[19] M. Safavi, E. Amani, A comparative study of turbulence models for non-premixed swirl-stabilized flames, J. Turbul. 19 (2018) 1017–1050.
[20] D.A. Lysenko, I.S. Ertesvåg, K.E. Rian, Numerical simulation of non-premixed turbulent combustion using the eddy dissipation concept and comparing with the steady laminar flamelet model, Flow, Turbul. Combust. 93 (2014) 577–605.
[21] M. Abdollahzadeh, J.C. Páscoa, P.J. Oliveira, Numerical Modeling of Boundary Layer Control Using Dielectric Barrier Discharge, in: Conferência Nac. Em Mecânica Dos Fluidos, Termodinâmica E Energ. MEFTE, 2012: pp. Paper No 61, 1–10.
[22] Y.B. Suzen, P.G. Huang, Simulations of flow separation control using plasma actuators, in: 44th AIAA Aerosp. Sci. Meet., Reno, Nevada, 2006: p. 877.
[23] A. Bouchmal, Modeling of Dielectric-Barrier Discharge Actuator, Delft University of Technology, Master of Science Thesis, 2011.
[24] H. Borradaile, K. Kourtzanidis, F. Rogier, K.S. Choi, X. Mao, Flow reversal in millimetric annular DBD plasma actuator, J. Phys. D. Appl. Phys. 54 (2021) 345202.
[25] Y. Tong, X. Liu, S. Chen, Z. Li, J. Klingmann, Effects of the position of a bluff-body on the diffusion flames: A combined experimental and numerical study, Appl. Therm. Eng. 131 (2018) 507–521.
[26] J.A. Denev, J. Fröhlich, H. Bockhorn, Evaluation of mixing and chemical reactions within a jet in crossflow by means of LES, in: Proc. Eur. Combust. Meet., 2005.
[27] M. Khosravi, M. Javan, Three-dimensional features of the lateral thermal plume discharge in the deep cross-flow using dynamic adaptive mesh refinement, Theor. Comput. Fluid Dyn. 36 (2022) 405–422.
[28] M.A. Azim, Mixing of co-axial streams: Effects of operating conditions, J. Appl. Fluid Mech. 9 (2016) 751–756.